Journal of Hazardous Materials 172 (2009) 330–337

Contents lists available at ScienceDirect

Journal of Hazardous Materials

journal homepage: www.elsevier.com/locate/jhazmat

Toxicity assessment from electro-coagulation treated-textile dye wastewaters by bioassays

Soraya M. Palácio[a], Fernando R. Espinoza-Quiñones[b,*], Aparecido N. Módenes[b], Cláudio C. Oliveira[a], Fernando H. Borba[b], Fernando G. Silva Jr.[b]

[a] Postgraduate Program of Chemical, Maringá State University, Av. Colombo 5790, 87020-900, Maringá, PR, Brazil
[b] Postgraduate Program of Chemical Engineering, Paraná West State University, rua da Faculdade 645, Jd. Santa Maria, 85903-000, Toledo, PR, Brazil

ARTICLE INFO

Article history:
Received 19 May 2009
Received in revised form 2 July 2009
Accepted 3 July 2009
Available online 10 July 2009

Keywords:
Textile dye
Electro-coagulation
Factorial design
*Bio*assays

ABSTRACT

In this study the pollutant removal from a textile dyeing wastewater has been investigated by using the electro-coagulation technique with iron electrodes. In order to obtain optimal values of the system state variables, a 3^3 full factorial experimental design was applied. The electro-coagulation (EC) process response was evaluated on the basis of COD removal and decolourisation values. The electrolysis time and density current were statistically significant for the COD removal and decolourisation. Based on the lettuce seeds (*Lactuca sativa*) and brine shrimp (*Artemia salina*), the lowest toxicity level was achieved in 5 min of electrolysis time. Due to the remaining high toxicity level above 30 min of electrolysis time, the EC process is not adequate to be used in a single effluent treatment, suggesting that this electrochemical process of up to 5 min could be used as part of a complete effluent treatment system.

1. Introduction

Nowadays an integrated management of hydric resources, as well as the restoration of environmentally degraded areas, demand new technologies for pollution removal which will minimize the environmental impact, caused by toxic compounds released by industrial effluents and other residues. In particular, the contamination source by wastewater from textile dyeing is a significant source of environmental pollution [1].

In the last decade, the electro-coagulation technique (EC) has been applied to solving problems in wastewater treatment in order to ensure a good quality effluent before its disposal into aquatic environment. Due to its inherent simplicity of design and operation, together with the growing need for small-scale cost effective water treatment systems, the EC technology has received a renewed interest for industrial applications.

Reviews about the perspectives and possibilities of the EC technology for water treatment [2–4] have increased recently. Electro-coagulation has been successfully used to treat a wide range of organic and inorganic pollutants from different kinds of wastewater originated by the industrial metal processes [5,6], synthetic metal solution [7,8], wastewaters [9], alcohol distillery wastewater [10], and textile industry [11–14].

The purpose of this study was to investigate the pollutant removal from a textile dyeing wastewater by the application of the electro-coagulation technique with iron electrodes. In order to estimate the reactor efficiency the following criteria were used: chemical oxygen demand (COD), carbon organic total (COT), turbidity, total organic nitrogen, ammonia, nitrate, and chemical element concentration values. Based on the lettuce seeds (*Lactuca sativa*) and brine shrimp (*Artemia salina*), the toxicity of non- and treated effluent was estimated.

2. Materials and methods

2.1. Sampling

A large amount of samples in several consecutive days was collected from an industrial laundry, where the wastewaters were the by products of cloths dyeing and the partly coloured-cloths dyeing removal, located in the city of Toledo (Brazilian Parana state). A mixture of all samples was made in order to obtain a homogenized non-treated industrial dyeing effluent (IDE). Before the electro-coagulation (EC) treatments, all IDE samples were preserved, according to the standard methodologies prescribed by American Public Health Association [15]. Small portions of non-treated IDE samples were used for characterization.

* Corresponding author. Tel.: +55 45 33797094; fax: +55 45 33797002.
E-mail addresses: f.espinoza@terra.com.br, espinoza@unioeste.br (F.R. Espinoza-Quiñones).

0304-3894/$ – see front matter © 2009 Elsevier B.V. All rights reserved.
doi:10.1016/j.jhazmat.2009.07.015

2.2. EC reactor

A laboratory-scale EC reactor consisting of 1.5 L glass cylindrical container with a 11 cm diameter and 15 cm height was used. Eight iron plates with a 5 cm width, 11 cm height, and 0.15 cm thickness were used as electrodes. In the upper part of the EC reactor, the iron electrode plates were firmly assembled in an upright position and arranged parallel to each other, with a gap of 0.5 cm between the anode and cathode plates, using a non-conducting horizontal support to avoid any short-circuits. The electrodes were dipped into the beaker containing the IDE effluent with a 1.0 L working volume. The active electrode surface area was 0.035 m^2. The electrodes were operated in a mono-polar mode and were connected to terminals of direct current power supply (Instrutemp DC Power Supply, FA 1030), which contained an internal digital ammeter and voltmeter, that provided the stabilized currents and voltages, ranging from 0 to 10 A, and from 0 to 30 V, respectively. During the experiments the direction of the current was reversed every 30 min in order to limit the formation of passive layers [2].

2.3. Chemicals and sample preparation

The chemicals used were of analytical-reagent grade. A set of 1.0 g L^{-1} stock solutions of Solophenyl orange TGL ($C_{25}H_{33}ClN_6O_6S_2$), Solophenyl blue 71 ($C_{40}H_{23}N_7Na_4O_{13}S_4$), Solophenyl scarlet BNLE ($C_{44}H_{32}N_{10}Na_4O_{16}S_4$), Solophenyl yellow ARL ($C_{48}H_{26}N_8Na_6O_{18}S_6$), Solophenyl black FR ($C_{44}H_{32}N_{13}Na_3O_{11}S_3$) e Navy Blue 98 ($C_{38}H_{24}N_5Na_3O_{13}S_3$) was prepared from their direct dye standard powder using distilled water. Molecular absorption spectra were measured from diluted pure dyeing solutions (50 mg L^{-1}) in order to identify the maximum absorption wavelength. From this stock solution a mixture of dyeing standards was also prepared, resulting in a final dyeing concentration of 8.33 mg L^{-1} and then a sufficient amount of NaCl was added in order to reach the same conductivity value (16.88 mS cm^{-1}) of the IDE samples for posterior EC measurements.

Certified iron standard solutions (1.0 g L^{-1} for AAS, Merck) were used to obtain the calibrated curve for atomic absorption spectrometer.

In order to obtain the sensibility curves for SR-TXRF (Synchrotron Radiation Total Reflection X-ray Fluorescence) spectrometer, several mixtures of multi-elemental standards (from a set of mono-element standards (1.0 g L^{-1} for AAS) were used at different concentrations. For SR-TXRF analysis, a 2 mL aliquot of each filtered sample was taken and a 20 μL standard solution (1.0 g Ga L^{-1}) was added as an internal standard. Afterwards, an aliquot of 5 μL was deposited on a pre-cleaned acrylic disk (Ø 30 mm and 3 mm tick) and dried at room temperature. The same procedure was repeated for the multi-elemental standards at five different concentrations. All the disk-samples were prepared in triplicates, except for the standard ones, which were in quintuplicate.

2.4. Batch experiments

Before each EC experiment, the pH adjustments of IDE and dyeing standard solutions were done with NaOH (6 M) and H_2SO_4 (3 M). In a typical run, performed at room temperature, 1L IDE sample was placed in the EC reactor. Due to the low dyeing standard solution conductivity, it was not necessary to add NaCl to increase the current. Before each experiment, the oxide and/or passive layers from the electrodes were removed, rinsed and dried. The solution was slowly stirred. For the applied 1–2 V voltage ranges of the reactor electrodes, high current densities have been established (28.6–142.9 A m^{-2}) and thus high bubble densities could be reached, allowing both coagulation and flotation processes to take place in the polluted media [4]. The chemical reactions taking place at the anode are given below [2,3].

For iron anode:

$$Fe_{(s)} \rightarrow Fe^{2+}_{(aq)} + 2e^-, \quad (1)$$

$$Fe^{2+}_{(aq)} + 2OH^-_{(aq)} \rightarrow Fe(OH)_{2(s)} \quad (2)$$

At cathode

$$2H_2O_{(l)} + 2e^- \rightarrow H_{2(g)} + 2OH^-_{(aq)}, \quad (3)$$

In textile industry a large quantity of contaminants such as unreacting dyes, suspended solids, dissolved solids, and other auxiliary chemicals (NaCl, Na_2CO_3 and Na_2SO_4) are generated. In EC process, it is expected that the generated Fe ions undergo further spontaneous reactions to produce corresponding hydroxides and/or polyhydroxides. These complexes have strong affinity for dispersed particles as well as counter ions to cause coagulation [3]. Four main mechanisms, such as surface complexation, electrostatic attraction, chemical modification, and precipitation, have been suggested to describe the process by which contaminants are removed from wastewater using the EC system [12].

The presence of chloride ions strongly catalyses the conversion of pollutant organic compounds to innocuous compounds such as CO_2 and H_2O [16]. At the anode, an electrochemical reaction of chloride ion can be represented as

$$2Cl^- \rightarrow Cl_{2(g)} + 2e^- \quad (4)$$

Moreover, it could be presumed that other oxidizing agents such as nascent oxygen, ozone, hydrogen peroxide, and free radicals such as $ClO^\bullet$, $Cl^\bullet$, and $OH^\bullet$ are generated during the electrolysis [17]. In addition, there is oxygen evolution reaction

$$2H_2O \rightarrow O_2 + 4H^+ + 4e^- \quad (5)$$

The cathodic conversion of molecular oxygen to active oxygen in the presence of chloride ion [16] can be represented as

$$2H_2O + 2O_{2(aq)} + 4e^- \rightarrow 2H_2O_2 + 4OH^- \quad (6)$$

Since the solubility of oxygen and ozone in water is very less, it is presumed that HOCl and H_2O_2 are the main oxidants that are responsible for degradation of organics, generating secondary pollutants, such as ammonia and nitrate ions [14]. The electrochemical reduction of nitrate ions can be represented as

$$NO_3^- + 3H_2O + 5e^- \rightarrow 0.5N_2 + 6OH^- \quad (7)$$

$$NO_3^- + 6H_2O + 8e^- \rightarrow NH_3 + 9OH^- \quad (8)$$

The direct and indirect electrochemical oxidation of ammonia in the presence of hydroxyl and chloride ions can be represented as

$$2NH_3 + 6OH^- \rightarrow N_2 + 6H_2O + 6e^- \quad (9)$$

$$2NH_3 + 6Cl^- \rightarrow N_2 + 6HCl + 6e^- \quad (10)$$

After each experiment, the floated and precipitated materials were withdrawn and the clarified effluent sample was pipetted out from the reactor, and then allowed to settle for a few hours in a polyethylene flask. Finally, the clarified supernatant liquid was collected and preserved according to the Standard Methods [15], and stored for characterization.

2.5. Factorial design

The influence of three reactor operating parameters (ROP): initial pH of the IDE solution, electrolysis time and current density were investigated in order to improve the COD removal and decolourisation efficiencies, according to the 3^3 full factorial experimental designs with three replicates. The three levels of each ROP

Table 1
Assigned levels for three reactor operating parameters.

ROP	Variables	Assigned levels		
		-1	0	+1
Electrolysis time (min)	q_1	15	30	45
Initial pH	q_2	3	7	11
Current density ($A\,m^{-2}$)	q_3	28.6	85.7	142.9

were chosen from previous preliminary tests and the know-how as summarized in Table 1. In the analytical EC process, where ROP values could influence an experimental response in terms of COD removal and decolourisation values, the estimated 3-D graphical response is expected to be a certain function of the parameter levels, allowing the optimization of the ROP values by applying the Lagrange criteria [18]. An ANOVA analysis permits to assess what kind of interaction between the ROP are statistically significant to the response function.

2.6. Measurements

All physicochemical parameter measurements were made by applying the Standard Methods [15] for each non- and treated IDE sample. The chemical oxygen demand was determined by the open reflux/titrimetric method. The pH was measured by using a digital pH meter (Tecnal TEC-2). Turbidity (Nephelometric Turbidity Unit, NTU) was determined with a turbidimeter Tecnal, model TB1000. Conductivity was measured by using a conductivity meter (Tecnal R-TEC-04P-MP). A total organic carbon (TOC) analyzer (model 5000-A, Shimadzu) was used to measure the TOC of the solutions. Organic and ammonia nitrogen and inorganic nitrate contents were measured in order to characterize the IDE after the EC treatment. The amounts of inorganic nitrate were measured by using the kinetic cadmium-reduction method, while a colorimetric method based on the phenate–hypochlorite reaction was used in order to determine the organic and ammonia nitrogen content. The oxidized products and the reduction in dye concentration were measured by using a UV–visible Spectrophotometer (Shimadzu UV-1610PC). From the average of absorbance values obtained from triplicate samples, the decolourisation value (ΔAbs) was calculated by the Eq. (11).

$$\Delta\mathrm{Abs}(\%) = 100\frac{[\mathrm{Abs}_0^{\mathrm{M}} - \mathrm{Abs}^{\mathrm{M}}]}{\mathrm{Abs}_0^{\mathrm{M}}} \tag{11}$$

where $\mathrm{Abs}^{\mathrm{M}}$ is the average of absorbance values at the maximum visible absorbency wavelength. $\mathrm{Abs}_0^{\mathrm{M}}$ and $\mathrm{Abs}^{\mathrm{M}}$ correspond to the values before and after the EC treatment, respectively.

The whole sludge formed, as a by-product of the EC process, was weighed before and after a drying process. Then it was treated by an acidic digestion procedure by using an AAS spectrometer (model AA 932–GBC, Analitica) in order to determine the amount of iron in it.

The SR-TXRF measurements were performed using a polychromatic X-ray beam, with 20 keV maximum energy, from the D09-XRF beam line at the Brazilian Light Synchrotron Laboratory (LNLS). Each reflector disk-sample was positioned for the total reflection condition, and the acquisition time was set at 100 s. For X-ray detection, a HP-Ge detector with 160 eV FWHM@Mn-Kα line was used. All X-ray spectra were analyzed using the AXIL program [19]. An exponential-type function was fitted in good agreement ($r^2 = 0.9972$ and $\chi^2 = 0.0068$) with the relative-to-gallium sensitivity experimental data for light elements (see Eq. (12)). The element concentrations in liquid samples were determined by the Eq. (13).

$$S_{\mathrm{r}}(Z) = \exp\left(-22.811 + 1.438 \times Z - 0.0227 \times Z^2\right) \tag{12}$$

$$C(Z) = \frac{I_Z}{I_{\mathrm{Ga}}} \times \frac{C_{\mathrm{Ga}}}{S_{\mathrm{r}}(Z)} \tag{13}$$

where Z is the atomic number ranging from 14 to 40; I – represents the fluorescent intensity of the element; $C\,(\mathrm{mg\,L^{-1}})$ – represents the concentration of the element in the liquid phase; and C_{Ga} – stands for the internal standard concentration ($10\,\mathrm{mg\,Ga\,L^{-1}}$).

2.7. Toxicological test

In order to assess the non- and treated IDE toxicological response on living organisms, lettuce seeds (*L. sativa* L.) and brine shrimp (*A. salina*) were used as toxicity level bioindicators due to their fast response to concentrated and diluted by-product solutions. Bioassays in lettuce (*L. sativa* L.) seeds were conducted for germination index (IG), length of the radicle and length of hypocotyl structure, following the methodology proposed by Sobrero and Ronco [20]

The AG and GI for bioassays, containing 20 lettuce seeds each, at five diluted IDE doped with nutritive solution, in triplicate, were calculated (using Eqs. (14) and (15)), from the germination of lettuce seeds (*L. sativa* L.) in both the diluted treated IDE doped hard water solution and a non doped one as a control.

$$\mathrm{AG} = \frac{N_{\mathrm{germ}}}{N_{\mathrm{seed}}} \tag{14}$$

$$\mathrm{GI} = \frac{N_{\mathrm{germ}}}{N_{\mathrm{cont}}} \times \frac{\mathrm{RL}_{\mathrm{germ}}}{\mathrm{RL}_{\mathrm{cont}}} \tag{15}$$

where, N_{germ} is the average number of germinated seeds in the diluted treated IDE doped nutritive solution; N_{seed} is the total number of seeds; and N_{cont} is the average number of germinated control seeds in the non-doped-nutritive solution. $\mathrm{RL}_{\mathrm{germ}}$ is the average root length of germinated seed in the diluted treated IDE doped-nutritive solution, and $\mathrm{RL}_{\mathrm{cont}}$ – the average root length of germinated seed in the non doped-nutritive solution.

For each IDE sample, mixtures of IDE sample and reconstituted hard water (v/v) were prepared for five dilutions (1%, 3%, 10%, 30% and 100%) of non- and treated IDE solutions in triplicates. In the present work, twenty lettuce seeds have been put on the filtration-type papers containing diluted IDE solutions in Petri plates and properly covered against the environment. Then they were germinated inside an incubator, at a $22 \pm 2\,^{\circ}\mathrm{C}$ constant temperature, during 120 h. This procedure was repeated three times.

A brine shrimp (*A. salina* L.) assay was also applied in order to perform a screening for the lethality of the non- and treated IDE solutions based on the LC_{50} criterion. Using a nutritive solution described by Meyer [21], the cist-like eggs hatch within a few hours and the more resistant nauplii were used in the toxicity assay. For each IDE sample, 5 mL of a mixture of IDE sample and nutritive solutions (v/v) were prepared in 10 mL glassware for five dilutions (20%, 40%, 60%, 80%, and 100%) of non- and treated IDE solutions in triplicates, where 10 larvae of *A. salina* L. were incubated at room temperature and light regime, during 24 h, and then the LC_{50} was calculated. As a control assay 10 larvae of *A. salina* L. were incubated in a pure nutritive solution.

3. Results and discussion

3.1. Non-treated IDE and dyeing standard characterization

The typical characteristics of non-treated IDE are presented in Table 2. The maximum absorption wavelength for each diluted pure dyeing solution was identified to be equal to 404, 416, 483, 494.5 and 588 nm for Solophenyl yellow, Solophenyl orange, Solophenyl black, Solophenyl scarlet, and Solophenyl blue, respectively, while the absorbance values for the mixture of a standard dyeing solution at the same wavelengths were measured to be 4.43 (404 nm),

Table 2
Physico-chemical characteristics and element concentrations of natural IDE.

Parameter	Value	Element	Concentration (mg L^{-1})
pH	12.5 ± 0.2	S	878 ± 44
Turbidity (NTU)	306 ± 9	Cl	3811 ± 190
Organic nitrogen (mg L^{-1})	4.6 ± 0.1	Ca	98 ± 5
Ammonia nitrogen (mg L^{-1})	1.3 ± 0.1	Fe	1.11 ± 0.06
COD (mg L^{-1})	1636 ± 47	Cu	1.84 ± 0.09
Sulfate (mg L^{-1})	2681 ± 30		

4.45 (416 nm), 3.42 (483 nm), 3.29 (494.5 nm), and 2.99 (588 nm). In addition, the average of absorbance values for non-treated IDE sample were calculated to be 1.54 (404 nm), 1.51 (416 nm), 1.39 (483 nm), 1.39 (494.5 nm), and 0.96 (588 nm).

3.2. Statistical analysis

The results obtained for a 3^3 full factorial experimental design for the IDE samples are given in the Table 3, where the COD removal yield varies between 40% and 90%, while the decolourisation ranges between 6% and 100%, which are the values of a set of decolourisation yields at five maximum absorption wavelengths. In order to explain the behavior of COD removal and decolourization yield with the combined actions of ROP, two predicted models have been found in terms of linear and interaction coefficients, according to the Eq. (16), resulting in a good fitting between the predicted and observed values for COD removal and decolourisation, as shown in Fig. 1.

$$R = a_0 + \sum_{i=1}^{N} a_i q_i + \sum_{i=1}^{N}\sum_{j=1}^{N} b_{ij} q_i q_j + \sum_{i=1}^{N}\sum_{j=1}^{N}\sum_{k=1}^{N} w_{ijk} q_i q_j q_k + \sum_{i=1}^{N}\sum_{j=1}^{N} v_{ij} q_i^2 q_j^2 \quad (16)$$

where R is the experimental response; q is the set of ROP values, a_0 is a constant; a is a set of coefficients of the linear terms, b, w, and v are a set of coefficients associated with the linear and quadratic interactions between the ROP values, and N is the number of ROP.

The experimental response, based on the COD and decolourisation yield values, permitted the development of a statistical model, with a set of linear and quadratic coefficients associated with the ROP values, as summarized in Tables 4 and 5. The significance of the ROP effects and their possible combined actions were checked out by applying a two-way ANOVA analysis, using the Statistica® software, as shown in Tables 6 and 7.

Table 3
A 3^3 full factorial design with three replicates.

Run	q_1	q_2	q_3	COD removal (%)			Decolourisation (%)		
	(min)		(A m^{-2})	COD_1	COD_2	COD_3	Dec_1	Dec_2	Dec_3
1	15	3	28.6	77.1	76.0	76.2	5.8	6.0	6.2
2	15	3	85.7	74.6	73.7	74.4	72.5	76.3	80.1
3	15	3	142.9	78.2	77.0	77.6	93.9	96.8	99.7
4	15	7	28.6	75.2	76.2	75.7	62.7	63.3	63.9
5	15	7	85.7	74.5	73.2	73.7	93.4	95.3	97.2
6	15	7	142.9	69.4	70.5	69.9	73.2	75.5	77.8
7	15	11	28.6	42.2	41.1	41.8	14.5	14.6	14.7
8	15	11	85.7	52.9	51.2	52.1	21.2	23.6	26.0
9	15	11	142.9	54.0	55.4	54.8	64.4	67.1	69.8
10	30	3	28.6	80.1	80.8	80.4	59.5	59.8	60.1
11	30	3	85.7	77.8	75.2	76.3	91.5	93.4	95.3
12	30	3	142.9	82.8	81.2	81.7	96.7	97.7	98.7
13	30	7	28.6	76.8	74.9	74.6	81.9	85.3	86.2
14	30	7	85.7	80.7	82.5	82.2	95.8	97.8	98.3
15	30	7	142.9	81.7	79.8	80.9	99.7	97.7	98.7
16	30	11	28.6	45.0	45.4	43.9	32.2	32.5	33.2
17	30	11	85.7	68.8	67.2	68.5	66.1	66.8	67.5
18	30	11	142.9	68.9	67.4	68.0	78.4	78.8	80.0
19	45	3	28.6	82.8	83.5	82.5	71.7	72.1	73.2
20	45	3	85.7	79.7	80.4	80.1	97.9	98.4	99.9
21	45	3	142.9	88.3	87.2	87.7	98.0	98.5	100.0
22	45	7	28.6	75.2	76.5	75.7	95.9	96.4	97.8
23	45	7	85.7	81.9	82.9	82.9	97.0	97.5	99.0
24	45	7	142.9	83.0	81.9	81.7	98.9	97.9	99.4
25	45	11	28.6	46.8	45.2	46.3	44.8	43.9	45.2
26	45	11	85.7	71.9	69.9	70.2	77.2	75.7	78.0
27	45	11	142.9	74.9	75.6	75.4	94.6	92.7	95.5

Table 4
A set of linear and interaction coefficient values of the predicted model for COD removal with a 95% significance level ($p < 5\%$) and $r^2 = 0.9824$.

Parameter actions	Coefficient	Value	Standard deviation	t_{exp}	p (%)
q_0	a_0	70.208	0.320	219.22	<0.01
q_1	a_1	4.134	0.392	10.54	<0.01
q_2	a_2	−15.153	0.392	−38.63	<0.01
$(q_2)^2$	b_{22}	4.148	0.340	12.21	<0.01
q_3	a_3	6.709	0.453	14.80	<0.01
$(q_3)^2$	b_{33}	2.323	0.392	5.92	<0.01
$q_1 \times q_2$	b_{12}	1.752	0.277	6.32	<0.01
$q_1 \times (q_2)^2$	w_{122}	−0.986	0.240	−4.11	0.01
$(q_1)^2 \times q_2$	w_{112}	0.959	0.240	3.99	0.01
$q_1 \times q_3$	b_{13}	3.732	0.555	6.72	<0.01
$q_1 \times (q_3)^2$	w_{133}	1.061	0.481	2.21	3.09
$(q_1)^2 \times q_3$	w_{113}	1.407	0.481	2.93	0.48
$(q_1)^2 \times (q_3)^2$	v_{13}	0.927	0.416	2.23	2.95
$q_2 \times q_3$	b_{23}	11.233	0.555	20.24	<0.01
$q_2 \times (q_3)^2$	w_{233}	6.385	0.481	13.28	<0.01
$(q_2)^2 \times q_3$	w_{223}	−2.228	0.480662	−4.63	<0.01

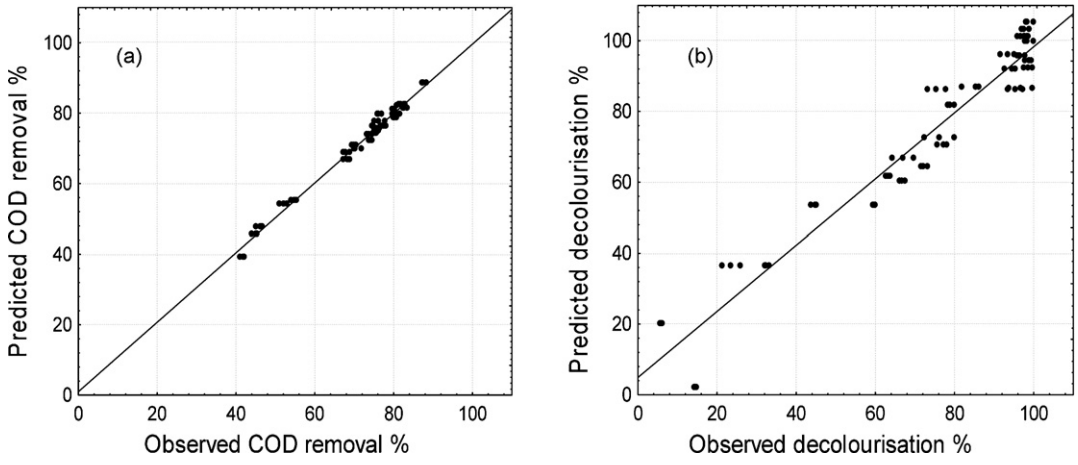

Fig. 1. Correlation between the observed COD removal (a) and decolourisation (b) values and their corresponding ones as predicted by the proposed statistical model.

Table 5
A set of linear and interaction coefficient values of the predicted model for decolourisation with a 95% significant level ($p < 5\%$) and $r^2 = 0.93424$.

Parameter actions	Coefficient	Value	Standard deviation	t_{exp}	p (%)
q_0	a_0	67.989	1.546	43.97	<0.01
q_1	a_1	15.895	1.894	8.39	<0.01
q_2	a_2	−5.407	1.894	−2.85	0.58
$(q_2)^2$	b_{22}	11.028	1.640	6.72	<0.01
q_3	a_3	28.000	2.188	12.80	<0.01
$(q_3)^2$	b_{33}	9.545	1.895	5.04	<0.01
$q_1 \times (q_2)^2$	w_{122}	−3.458	1.159	−2.98	0.41
$q_1 \times q_3$	b_{13}	−8.588	2.680	−3.20	0.21
$q_2 \times q_3$	b_{23}	−9.136	2.680	−3.41	0.11
$q_2 \times (q_3)^2$	w_{233}	−8.584	2.321	−3.70	0.05
$(q_2)^2 \times q_3$	w_{223}	−9.497	2.321	−4.10	0.01

Based on a total of 27 EC runs, response functions (R) were built in 3D graphs, and the experimental data were predicted by using a fourth order model (see Eq. (11)) for decolourisation and COD removal values, showing thus their dependencies on the ROP values. From the Tables 6 and 7, the ANOVA analysis has confirmed that both predicted models based on the Eq. (16), with coefficient values given in Tables 4 and 5, have reproduced very well the COD removal and decolourisation data. The ANOVA analysis has given confidence levels of 99.99% and 96.4%, when the significance level, calculated from the ratio of the mean square errors due to the regression and to the residues, is ranging from 0.01 to 3.6.

The statistical analysis of the 3^3 full factorial design have shown that the ROP values have significantly influenced the COD removal and decolourisation, according to the estimated a_1, a_2 and a_3 coefficient values. A negative effect ($a_2 < 0$, see Tables 4 and 5) is only assigned to the initial pH, suggesting an increase on the pollutant removal efficiency as the initial pH value is in alkaline region. Similar results were observed for the quadratic terms ($b_{22} > 0$ and $b_{33} > 0$, see Tables 4 and 5) on the initial pH and current density. It is a well known fact that EC processes are strongly pH dependent, because iron ions are difficult to aggregate under acidic conditions. While complexes such as iron hydroxides can be formed at alkaline pH, and at high initial pH conditions they are expected to shift the final pH towards alkaline region due to the generations of hydroxyl radicals. When electrolysis time and current density have simultaneously reached their higher levels, the COD removal and decolourisation were found at maximum values.

The combined actions of electrolysis time and initial pH ($q_1 \times q_2$), of initial pH and current density ($q_2 \times q_3$, $b_{23} = 11.233$), as well as, of electrolysis time and current density ($q_1 \times q_3$, $b_{13} = 3.732$), have significantly influenced ($p < 0.01\%$) only the COD removal (see Table 4). However, the colour removal is improved under the quadratic contribution of initial pH ($b_{22} = 11.028$, $p < 0.01\%$) and current density ($b_{33} = 9.545$, $p < 0.01\%$) and as a linear contribution of electrolysis time ($a_1 = 15.895$, $p < 0.01\%$), initial pH ($a_2 = -5.407$, $p < 0.58\%$), and current density ($a_3 = 28.0$, $p < 0.01\%$), as shown in Table 5. The colour removal has been significantly influenced by the combined action of electrolysis time and current density ($b_{13} = -8.588$, $p = 0.21\%$), as well as, of initial pH and current density ($b_{23} = -9.136$, $p = 0.11\%$). As can be observed in the Fig. 2, the best results for decolourisation were for pH 7 and high current density ($149\ A\ m^{-2}$).

3.3. Electrolysis time effect

Based on the 3^3 full factorial design and two-way ANOVA results, different EC experiments were performed, where the reactor performance was as follows: $142.9\ A\ m^{-2}$ current density, and pH 7. For this experimental set up, the electrolysis time ranging between 15 and 90 min has shown a good efficiency for the turbidity, sulphate, COD, and TOC, as can be seen in Fig. 3. After 15 min of EC treatment, the removal percentage of 92%, 62%, and 41% was reached for the turbidity, COD and TOC values, respectively. For the sulphate removal, a fast reduction around 75% in the first 5 min was observed to occur for the sulphates, keeping constant, within a standard deviation, for up to 90 min, while, constant removal values around 97%, 77%, and 55% were reached above 60 min of EC treatment for the turbidity, COD and TOC values, respectively. Moreover, an almost 100% decolourisation for IDE samples has been achieved above 30 min for all maximum absorption wavelengths, as shown in Fig. 4. Organic nitrogen, which is present in molecules of many organic materials, can be slowly destroyed by electrochemical processes, permitting a direct and indirect oxidation of organic matter in more simple forms, such as ammonia nitrogen, or inorganic nitrite and nitrate. During the EC process, a part of the total organic nitrogen has been flocculated to form a precipitated and floated matter and then a sludge, while the rest has been detected in a supernatant effluent. After about 5 min of electrolysis time, the nitrification process was observed to occur with the formation of ammonia nitrogen and then after 30 min the inorganic nitrate begins to be formed, as shown in Fig. 5. The reductions of S, Cl, Ca and Cu in 5–90 electrolysis time intervals are also summarized in Table 8.

3.4. Toxicological tests

The toxicological effect results of non-treated and treated IDE on the germination and root growth are summarized in Table 9. The estimated median lethal dose (LD_{50}) values and their confidence

Table 6
Two-way ANOVA test of the predicted model for COD removal values.

	Sum of square errors	Degrees of freedom	Mean square error	F		Significance level (%)
				Calculated	Statistical	
Regression	12397.5	18	688.7	248.864	1.8	<0.01
Residues	171.6	62	2.8			
Total	12569.1	80				

Table 7
Two-way ANOVA test of the predicted model for decolourisation values.

	Sum of square errors	Degrees of freedom	Mean square error	F		Significance level (%)
				Calculated	Statistical	
Regression	56828.3	18	3157.1	48.932	1.8	3.6
Residues	4000.3	62	64.5			
Total	60828.6	80				

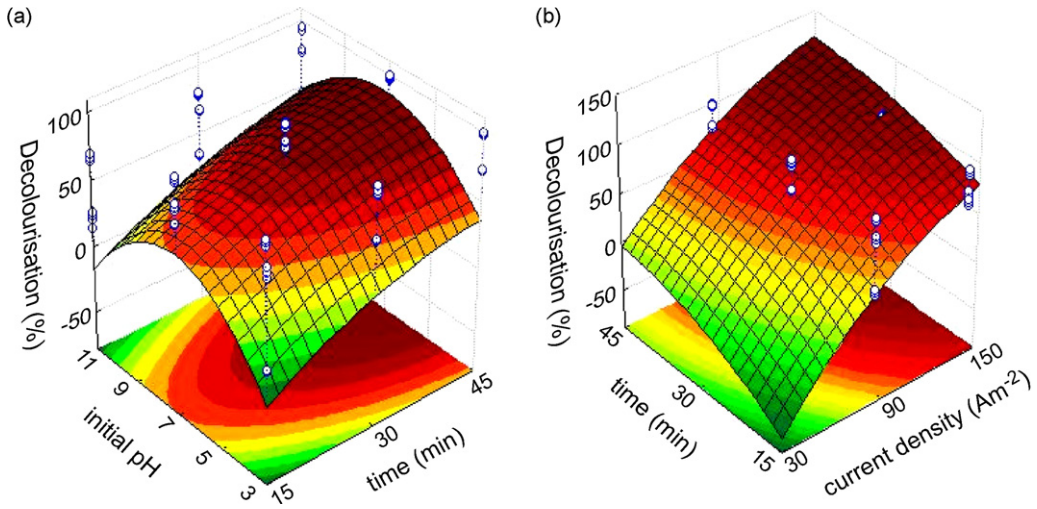

Fig. 2. Experimental response surface results obtained by applying a 3^3 full factorial design for the EC process, by using the treated IDE, from the experimental data of (a) decolourisation vs. electrolysis time (q_1) and initial pH (q_2) and (b) decolourisation vs. electrolysis time (q_1) and current density (q_3).

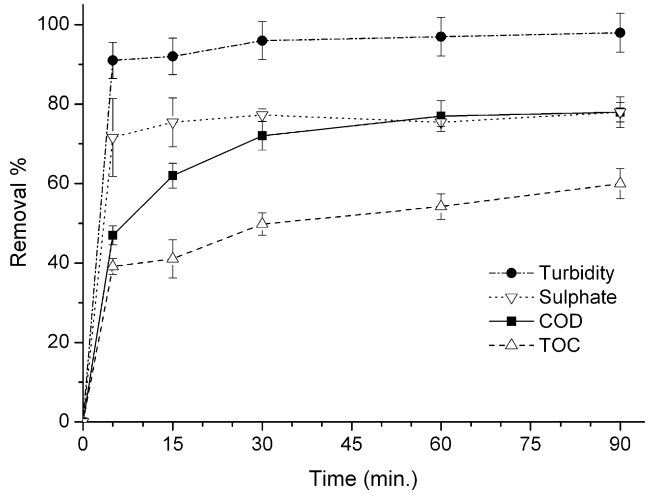

Fig. 3. Removal profiles (turbidity, sulfate, COD and TOC, %) as a function of electrolysis time for an EC system when using the non-treated IDE (initial pH 7.0), and the iron electrodes with 143 A m^{-2} current density.

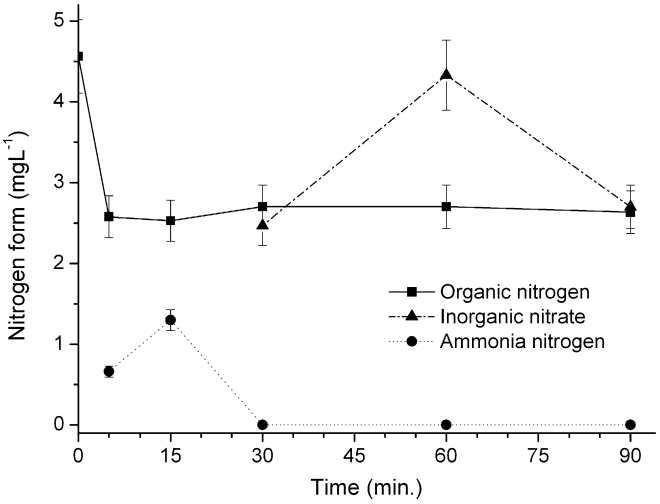

Fig. 5. Organic nitrogen, ammonia nitrogen, inorganic nitrate concentration as a function of electrolysis time for an EC system when using the non-treated IDE (initial pH 7.0), and the iron electrodes with 143 A m^{-2} current density.

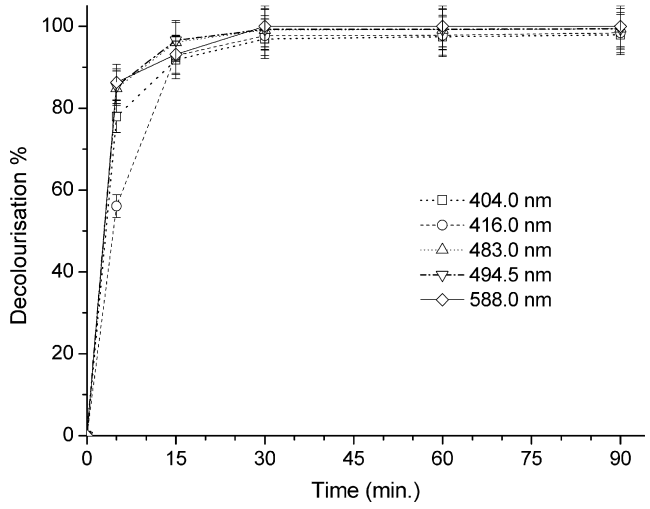

Fig. 4. The decolourisation profiles for all maximum absorption wavelengths as a function of electrolysis time for an EC system when using the non-treated IDE (initial pH 7.0), and the iron electrodes with 143 A m^{-2} current density.

intervals were derived by using the Trimmed Spearman-Karber method [22].

The length of the radicle and length of roots represented by the AG and GI were strongly inhibited by the presence of soluble toxic compounds in 100% non-treated IDE. The best results for the growth of the root and the root length were the 47% treated IDE solution at 5 min of electrolysis time, according to the best LD_{50} value (see Table 9). For high dose interval (10–30%) of treated IDE,

Table 8
Elementary removal percentage in the 5–90 min electrolysis time interval for the EC system, using the non-treated IDE (initial pH 7.0) and iron electrodes with 142.9 A m^{-2} current density.

Time (min)	Removal%			
	S	Cl	Ca	Cu
5	26	14	8	38
15	30	25	16	97
30	49	36	72	97
60	56	60	91	98
90	59	73	96	98

Table 9
The percentage of the absolute germination and the germination index average value for lettuce seed bioassays, calculated at five dilutions (1%, 3%, 10%, 30% and 100%) of non- and treated IDE solutions, in triplicates. The estimated median lethal dose (LD_{50}) values and their confidence intervals are derived by using the Trimmed Spearman-Karber method (Hamilton et al. [22]).

Time (min)	%Treated IDE solution mixed to control solution										LD_{50} (%)	Confidence interval (95.5%)
	1		3		10		30		100			
	AG[a]	GI[b]	AG	GI	AG	GI	AG	GI	AG	GI		
0	90	73	80	17	70	15	50	8	0	0	21	13–32
5	85	59	85	52	85	94	80	70	0	0	47	41–55
15	90	100	85	75	85	58	80	39	0	0	35	29–43
30	85	65	80	49	70	47	60	36	0	0	28	21–37
60	80	58	80	61	70	51	70	44	0	0	40	31–52
90	80	72	70	62	70	48	60	29	0	0	29	21–40

[a] Absolute germination.
[b] Germination index.

Table 10
Estimated median lethal dose (LD_{50}) values obtained from the *Artemia salina* assay using 10 larvae in triplicate, and applied to five diluted treated IDE solutions for five electrolysis times. The estimated median lethal dose (LD_{50}) values and their confidence intervals derived by the use of Trimmed Spearman-Karber method (Hamilton et al., [22]).

Time (min)	%Treated IDE solution mixed to control solution					LD_{50} (%)	Confidence interval (95.5%)
	20	40	60	80	100		
0	30/30	30/30	30/30	30/30	30/30		
5	7/30	7/30	8/30	10/30	22/30	90	85–96
15	8/30	8/30	9/30	10/30	25/30	87	79–96
30	11/30	11/30	12/30	16/30	23/30	77	64–94
60	11/30	12/30	16/30	16/30	27/30	64	47–87
90	9/30	9/30	14/30	16/30	27/30	70	61–99

higher AG and IG values were observed at 5 min of electrolysis time. When there is an increase in the electrolysis time, the IDE have worsened for the seed germination, as shown by the decrease of both toxicological indicator values, suggesting that an increase in electrolysis time above 5 min, the seed germination begins to worsen.

On the other hand, a similar response was observed for the *Artemia* assay as compared with the *Lactuca* assay, as shown in Table 10. At 5 min electrolysis time, the highest LD_{50} value was achieved at 90% treated IDE, indicating that there is a smaller dead index for treated IDE and all their dilutions. The toxicological inhibition effect for both bioassays are due to the formation of more toxic nitrogen forms created from the organic nitrogen by oxidation processes during the EC treatments (see Fig. 5).

Because of the high remaining toxicity level above 30 min of electrolysis time, the EC process is not adequate to be used as a single effluent treatment. However, for a short electrolysis time of 5 min, the EC process has simultaneously provided a great pollutant removal and a lowest toxic load, suggesting that this electrochemical process could be used as a part of a complete effluent treatment system, that contains a subsequent biological treatment stage, in order to release the lowest pollutant load into water bodies, according to the environmental norms.

4. Conclusion

The preliminary EC results based on the full factorial design have shown that the initial pH is not a significantly statistical parameter in a 95% confidence level. Hence, the EC system was operated close to the natural effluent pH (7.0), where satisfactory results were achieved. By increasing the electrolysis time, high removal factors have been reached in turbidity, sulphates, COD, TOC, decolourisation, Cl, Ca, Cu, and S concentrations. The toxicological tests, based on the *Lactuca* and *Artemia* assays, have shown a low toxicity level for the treated-textile dye wastewaters by using the EC process for 5 min of electrolysis time. Due to the high remaining toxicity level above 30 min of electrolysis time, the EC process is not adequate for use in a single effluent treatment one, suggesting that this electrochemical process could be used as part of a complete effluent treatment system, that contains a subsequent biological treatment stage in order to release the lowest pollutant load into water bodies, according to the environmental norms.

Acknowledgments

We gratefully acknowledge the Brazilian Light Synchrotron Laboratory (LNLS) for partial financing of this study through the 5877 project.

References

[1] E.G. Solozhenko, N.M. Soboleva, V.V. Goncharut, Decolourization of azo dye solutions by Fenton's oxidation, Water Res. 29 (1995) 2206–2210.
[2] G. Chen, Electrochemical technologies in wastewater treatment, Sep. Purif. Technol. 38 (2004) 11–41.
[3] M.Y.A. Mollah, P. Morkovsky, J.A.G. Gomes, M. Kesmez, J. Pargad, D.L. Cocke, Fundamentals, present and future perspectives of electrocoagulation, J. Hazard. Mater. B114 (2004) 199–210.
[4] P.K. Holt, G.W. Barton, C.A. Mitchell, The future for electrocoagulation as a localized water treatment technology, Chemosphere 59 (2005) 355–367.
[5] M. Kobya, C. Ciftci, M. Bayramoglu, M.T. Sensoy, Study on the treatment of waste metal cutting fluids using electro-coagulation, Sep. Purif. Technol. 60 (2008) 285–291.
[6] K. Bensadok, S. Benammar, F. Lapicque, G. Nezzal, Electrocoagulation of cutting oil emulsions using aluminum plate electrodes, J. Hazard. Mater. 152 (2008) 423–430.
[7] A.K. Golder, A.N. Samanta, S. Ray, Removal of trivalent chromium by electrocoagulation, Sep. Purif. Technol. 53 (2007) 33–41.
[8] I. Heidmann, W. Calmano, Removal of Zn(II), Cu(II), Ni(II), Ag(I) and Cr(VI) present in aqueous solutions by aluminium electrocoagulation, J. Hazard. Mater. 152 (2008) 934–941.
[9] H.A. Moreno-Casillas, D.L. Cocke, J.A.G. Gomes, P. Morkovsky, J.R. Parga, E. Peterson, Electrocoagulation mechanism for COD removal, Sep. Purif. Technol. 56 (2007) 204–211.
[10] Y. Yavuz, EC and EF processes for the treatment of alcohol distillery wastewater, Sep. Purif. Technol. 53 (2007) 135–140.
[11] O.T. Can, M. Kobya, E. Demirbas, M. Bayramoglu, Treatment of the textile wastewater by combined electrocoagulation, Chemosphere 62 (2006) 181–187.
[12] S. Raghu, C.A. Basha, Chemical or electrochemical techniques, followed by ion exchange, for recycle of textile dye wastewater, J. Hazard. Mater. 149 (2007) 324–330.

[13] M. Bayramoglu, M. Eyvaz, M. Kobya, Treatment of the textile wastewater by electrocoagulation Economical evaluation, Chem. Eng. J. 128 (2007) 155–161.
[14] G.B. Raju, M.T. Karuppiah, S.S. Latha, S. Parvathy, S. Prabhakar, Treatment of wastewater from synthetic textile industry by electrocoagulation–electrooxidation, Chem. Eng. J. 144 (2008) 51–58.
[15] APHA, AWWA, WPCF, Standard Methods for the Examination of Water and Wastewater, 21st ed., American Public Health Association, Washington, DC, 2005.
[16] R.M. Serikawa, M. Isaka, Q. Su, T. Usui, T. Nishimura, H. Sato, S. Hamada, Wet electrolytic oxidation of organic pollutants in wastewater treatment, J. Appl. Electrochem. 30 (2000) 875–883.
[17] L. Szpyrkowicz, S.N. Kaul, R.N. Neti, S. Satyanarayan, Influence of anode material on electrochemical oxidation for the treatment of tannery wastewater, Water Res. 39 (2005) 1601–1613.
[18] S.L.C. Ferreira, W.N.L. Santos, C.M. Quintella, B.B. Neto, J.M. Bosque-Sendra, Doehlert matrix: a chemomoetric tool for analytical chemistry—review, Talanta 63 (2004) 1061–1067.
[19] P. Van Espen, K. Janssens, I. Swenters, AXIL X-Ray Analysis software. Canberra Packard, Benelux, 1986.
[20] M.C. Sobrero, A. Ronco, Ensayo de toxicidad aguda con semillas de lechuga (*Lactuca sativa* L.). En: Ensayos Toxicológicos y Métodos de Evaluación de Calidad de Aguas, G. Castillo (Ed.), Ottawa, Canadá, 2004, pp. 71–79.
[21] B.N. Meyer, N.R. Ferrigni, J.E. Putnam, L.B. Jacobsen, D.E. Nichols, J.L. McLaughlin, Brine shrimp: a convenient general bioassay for active plant constituents, Planta Med. 45 (1982), pp. 35-34.
[22] M.A. Hamilton, R.C. Russo, R.V. Thurston, Trimmed Spearman Karber statistical method for estimating median lethal concentration in toxicity bioassays, Environ. Sci. Technol. 11 (1977) 714–719.